VPS VIBRATIONS IN PHYSICAL SYSTEMS
DOI: 10.21008/j.0860-6897.2023.1.12
Vibrations in Physical Systems, 2023, 34(1), 2023112

Experimental and CFD study of the selected acoustic helicoidal resonator as a final element of an air installation

Wojciech ŁAPKA[1], Piotr JAKUBOWSKI[2]

[1] Institute of Applied Mechanics, Faculty of Mechanical Engineering, Poznan University of Technology, Jana Pawła II 24, 60-965 Poznań, Poland
[2] Maritime Advanced Research Centre CTO S.A. Environmental Laboratories Division, The Vibroacoustic Laboratory, 65 Szczecińska Str., 80-392 Gdańsk, Poland

Corresponding author: Wojciech ŁAPKA, email: wojciech.lapka@put.poznan.pl

Abstract The work presents an analysis of the selected helicoidal resonator as the end element of the air installation. Laboratory tests of the acoustic pressure level were performed at the outlet of the air installation in a room for different flow speeds. The measurement methodology in accordance to standards PN-EN ISO 3741 and PN-EN ISO 5135, which describes the acoustic test facilities, instrumentation and procedures to be used for precision grade determination of sound power levels in octave or one-third-octave bands of a noise source in reverberation test rooms.. The numerical CFD tests show the shape of the air stream in the function of the distance from the installation outlet for different flow speeds. Due to the helicoidal shape of the analyzed acoustic helicoidal resonator, the air stream also turns, which can be used to effectively mix air in the room.

Keywords: acoustic resonator, experiments, duct acoustics, air diffusers, air-terminal device.

1. Introduction

Diffusers used in ventilation systems are used to introduce air into rooms in such a way as to obtain the required microclimate conditions in them. The designer of the mechanical ventilation system must take into account the correct selection of its end elements separating the air, without which effective ventilation cannot be obtained, even in the case of a correctly determined stream of ventilation air, proper design of air ducts and selection of the best quality elements of ventilation or air conditioning devices used for air treatment. There are many types of diffusers, such as supply grilles and nozzles, linear (slot) diffusers, swirl diffusers, floor diffusers, displacement diffusers, etc. They differ in the way air is distributed, dispersed and mixed in the ventilated space [1].

Particularly noteworthy is mixing ventilation, which is based on the assumption that air pollutants emitted in the room should be diluted as quickly and evenly throughout the entire space of the room and then removed from it. For this purpose, the air is blown in at a relatively high speed, causing the movement of practically all air in the room. This system is also characterized by similar values of temperature and air humidity at each point in the room. It is the possibility of obtaining acceptable thermal comfort conditions that is the main reason for the high popularity of this solution. The air is usually blown from the ceiling or from under the windows. The relatively high speed of air supply makes it necessary to select the diffusers very carefully in terms of the range and profile of the air stream in relation to the dimensions of the room [1]. In addition to experimental work under mixing ventilation [2, 3], numerical scientific research with the use of CFD (Computational Fluid Dynamics) on the effectiveness of indoor air diffusers and duct elements are also carried out [4, 5].

One of the duct components of the air installation may be an acoustic helicoidal resonator [6-13], which may be considered as a swirl diffuser when placed at its end. A helicoid resonator is an acoustic system composed of a hard helicoidal profile mounted axially on a cylindrical mandrel, also placed axially in a cylindrical duct. This solution is similar to Archimedes' screw, but the key proportions are the helix pitch s to the diameter of the cylindrical duct d, the mandrel diameter d_m, the thickness of the helicoidal profile g and the number of spiral turns n, which is usually smaller than 1. It is an element operating in a narrow frequency band. Figure 1a shows a schematic view of the helicoidal acoustic resonator with its basic dimensions marked, and Figure 1b shows an example of the transmission loss characteristics in of frequency domain for specific parameters of the acoustic system.

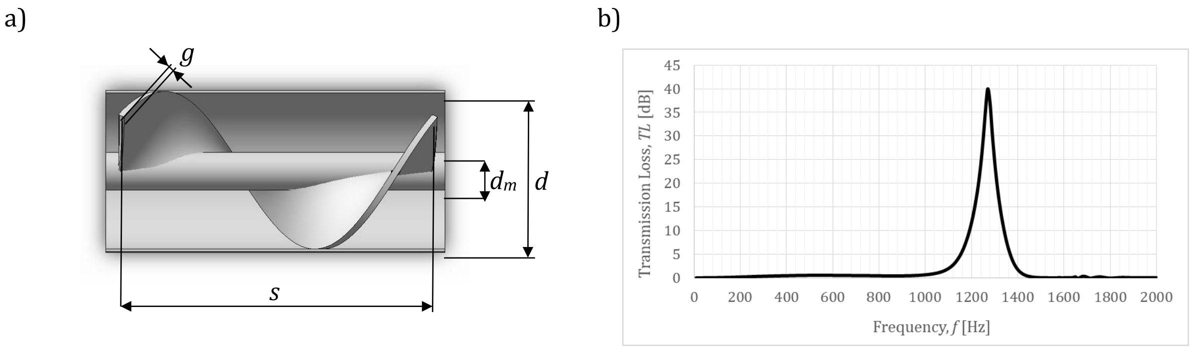

Figure 1. Acoustic helicoidal resonator: a) basic parameters, b) example transmission loss (TL) for specific parameters of the acoustic system: d=0.125 m, s/d=1.976, d_m/d = 0.24, g/d=0.04, n=0.695.

In previous scientific works, there were considered many acoustical properties, as example tuning the acoustic helicoidal resonators inside duct by the use of a short flat bar [7], by the use of 90 degree elbow [8] and by the change of it's mandrel diameter [9]. Numerical and experimental investigations of insertion loss [10], as well as the acoustic field distribution at the outlet of the helicoidal resonator [11] and with an elastic profile [12] were performed. As a part of the flow tests, calculations of pressure losses were performed for various flow velocities [13]. Additionally, pilot studies of rotating helicoidal resonators under the influence of air stream were performed [14]. Therefore in this work are presented the analysis of the selected acoustic helicoidal resonator as the end element of the air installation.

2. Experimental measurements

Tests for determining the acoustic power from air-terminal devices, air-terminal units, dampers and valves and air conditioning valves generating noise during air flow / outflow are carried out in accordance with the PN-EN ISO 5135 standard [15], in which the method for determining the acoustic power is referred to in the PN-EN standard ISO 3741 [16] at the Maritime Advanced Research Centre CTO S.A. in Gdańsk.

To the reverberant measuring chamber in which the tested object is mounted (Fig. 1), connected to the duct to which a silent air blast is provided with the set flow parameters, so that the noise produced by the tested object meets the background noise criteria described in the PN-EN ISO 3741 standard.

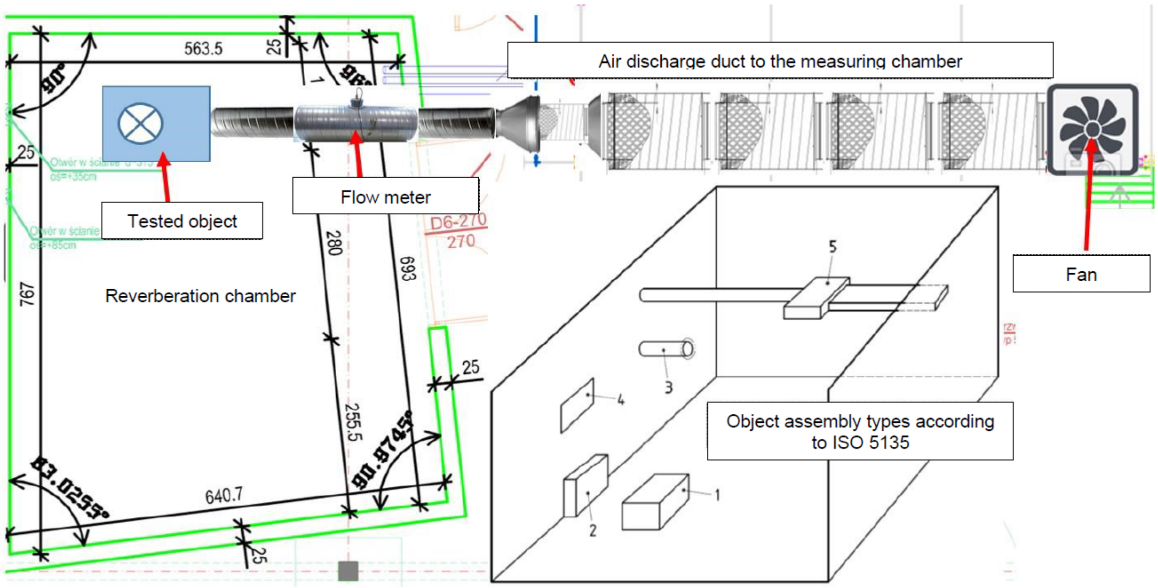

Figure 2. Illustrative diagram of the test set-up and laboratory room for measuring the acoustic power of air-terminal devices according to PN-EN ISO 5135 at the Maritime Advanced Research Centre CTO S.A.

The acoustic background is considered to be the sound pressure level of the noise coming from an open duct (i.e. with a disassembled object) with the given air flow parameters as during the test of the air connection object. The air blown into the measuring chamber during the tests flows out through venting holes designed for this purpose, ensuring free air flow. The result of the measurements will be the

 DOI: 10.21008/j.0860-6897.2023.1.12

characteristic of the acoustic power L_{WA} [dB] as a function of the air outflow velocity v [m / s]. In Figure 3 are presented the view inside reverberation chamber with example two microphones positions at the outlet of the cylindrical duct (diameter d=0.125 m, total length l=1,4 m) with the selected acoustic helicoidal resonator (n=0.695, s/d=1.976, d_m/d= 0.24, g/d=0.04) mounted inside at the distance of 0.287 m from the outlet. The measurements were performed with BRÜEL & KJÆR LAN-XI Data Acquisition Hardware Type 3052-A-030 with TYPE 4955, 1/2 "Low-Noise Free Field Microphones. There were six measuring points located throughout the reverberation chamber. The location of the acoustic helicoidal resonator at a distance of about two pipe diameters from the outlet is necessary for its proper operation – resonance. As presented in Figure 3a, the microphone positioned on the axis of the pipe outlet at a distance of 1 m was equipped with a nosecone for turbulent air-flow and the microphone positioned at an angle of 45° at a distance of 1 m had a typical windscreen. Test conditions in the reverberation chamber: temperature 22°C, relative air humidity ranging from 50% to 70%, atmospheric pressure ranging from 1005 hPa to 1012 hPa. The temperature of the supplied air in the installation ranged from 20°C to 21°C.

a) b)

Figure 3. The view inside reverberation chamber: a) example two microphones positions at the same horizontal level inside reverberation chamber at the outlet of the cylindrical duct (d=0.125 m), (b) the selected acoustic helicoidal resonator (n=0.695, s/d=1.976, d_m/d= 0.24, g/d=0.04) mounted inside at the distance of 0.287 m from the outlet.

In Figure 4 are presented the results of measured sound power levels according to ISO 5135 in one-third octave bands for selected acoustic helicoidal resonator (n=0.695, s/d=1.976, d_m/d= 0.24, g/d=0.04) and in table A are presented the total acoustic power levels, L_{WA} [dB], according to ISO 3741.

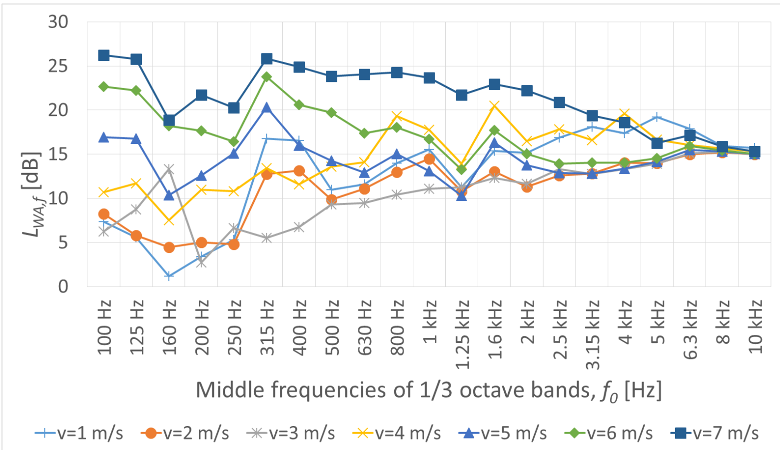

Figure 4. The results of measured sound power levels according to ISO 5135 and ISO 3741 in one-third octave bands, $L_{WA,f}$ [dB], for selected acoustic helicoidal resonator (n=0.695, s/d=1.976, d_m/d= 0.24, g/d=0.04) as the end element of the air system for seven different air flow velocities.

Based on the results of measurements of acoustic power levels in one-third octave bands, it should be concluded that for each considered flow velocity, lower levels are visible in the one-third octave band with a center frequency of 1250 Hz, which corresponds to the resonant frequency of the considered helicoidal resonator (in this case, 1270 Hz). Thus, the noise generated by the air flow is damped by the action of the helicoidal resonator.

Table 1. Total acoustic power levels, L_{WA} [dB], according to ISO 5135 and ISO 3741 measured for selected acoustic helicoidal resonator with parameters n=0.695, s/d=1.976, d_m/d= 0.24, g/d=0.04 as the air-terminal device. The expanded measurement uncertainty U = 4,1 dB.

Velocity, v [m/s]	1	2	3	4	5	6	7
Sound power level, L_{WA} [dB]	28.3	25.6	27.4	29.2	28.3	31.6	35.8

Total sound power levels generally tend to increase with increasing flow velocity with the exception of 1 m/s and 4 m/s, which are higher than the following levels. For the highest analyzed flow velocity, 7 m/s, the sound power levels are clearly higher in the individual one-third octave bands. This is due to greater airflow noise due to greater turbulence as the flow velocity increases.

3. CFD analysis and results

3.1. General description of CFD models

The Computational Fluid Dynamic (CFD) turbulent model were solved with the use of single-phase flow k-ω turbulence Reynolds-averaged Navier-Stokes (RANS) equations for conservation of momentum and the continuity equation for conservation of mass with compressible flow (Mach number less than 0.3) in COMSOL Multiphysics [18, 19, 20]. The main feature of this model is fluid properties, which adds the Navier-Stokes equations and the transport equations for the turbulent kinetic energy k and the specific dissipation ω. It provides an interface for defining the fluid material (here it is air) and its properties [18]. The fluid-air properties are: temperature 20ºC, reference pressure 1 atm, density and dynamic viscosity were calculated automatically from COMSOL material library module [18].

The boundary conditions (b.c.) used to calculate the considered models are described as:

- wall slip - there are no viscous effects at the slip wall at all hard surfaces of cylindrical duct, room wall and helicoidal resonator,
- normal inflow velocity at the inlet of the cylindrical duct in the range of air flow velocities from 0.5 m/s to 2 m/s
- open boundary conditions - no viscous stress at the outlet, pressure equals 0Pa.

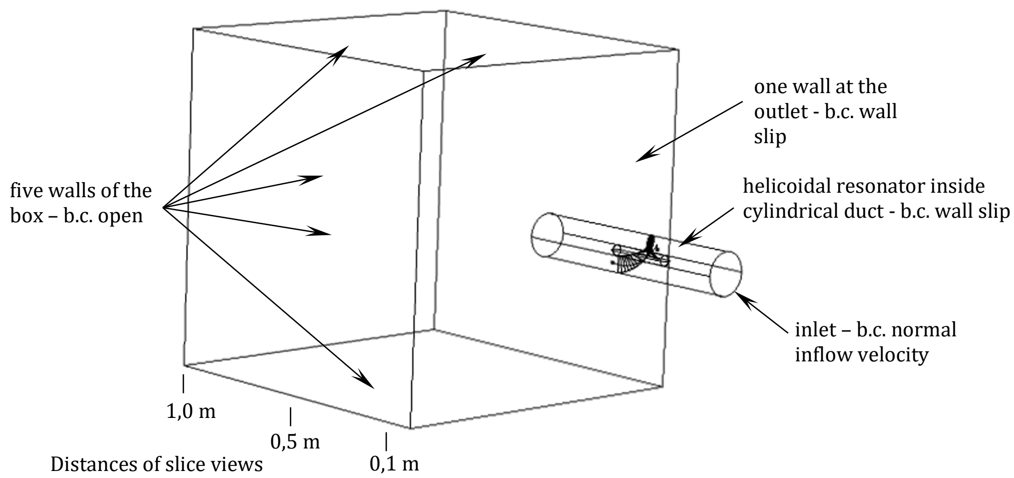

Figure 5. Description of the three dimensional (3D) CFD model of the cylindrical duct (d=0.125 m, l=0.7 m) with acoustic helicoidal resonator (n=0.695, s/d=1.976, d_m/d= 0.24, g/d=0.04) connected with outflow box of air of the dimensions 1.0 x 1.0 x 1.0 m.

As presented in Fig. 1, the geometrical three dimensional (3D) CFD models consist of 0.24 m in length of inflow cylindrical duct with the diameter d=0,125 m, the duct with helicoidal resonator (n=0.695, s/d=1.976, d_m/d= 0.24, g/d=0.04) equals 0.46 m in length, the same distance of 0.287 m as in experiment between duct outlet and resonator, and connected outflow box of air of the dimensions 1.0 x 1.0 x 1.0 m with one wall boundary condition at the resonator outlet and five open boundary conditions at the other box walls. Finite element mesh was generated automatically as a free tetrahedral and controlled by physics. The stationary solver was used.

3.2. CFD results

The numerical CFD calculations show the shape of the air stream in the function of the distance from the installation outlet for different flow speeds. The inflow air velocity speeds have been calculated in the range most favored in ventilation with regard to noise levels at the outlet of air-terminal devices and it was from 0.5 m/s to 2.0 m/s. In figure 6 are presented the slice views of air velocity inside 3D 1m cubic box at the outflow side of cylindrical duct with resonator calculated for flows with three air velocities, which equalled 0.5 m/s, 1 m/s and 2 m/s, and for three distances from the outlet of the cylindrical duct with helicoidal resonator, that equalled 0.1 m, 0.5 m and 1 m.

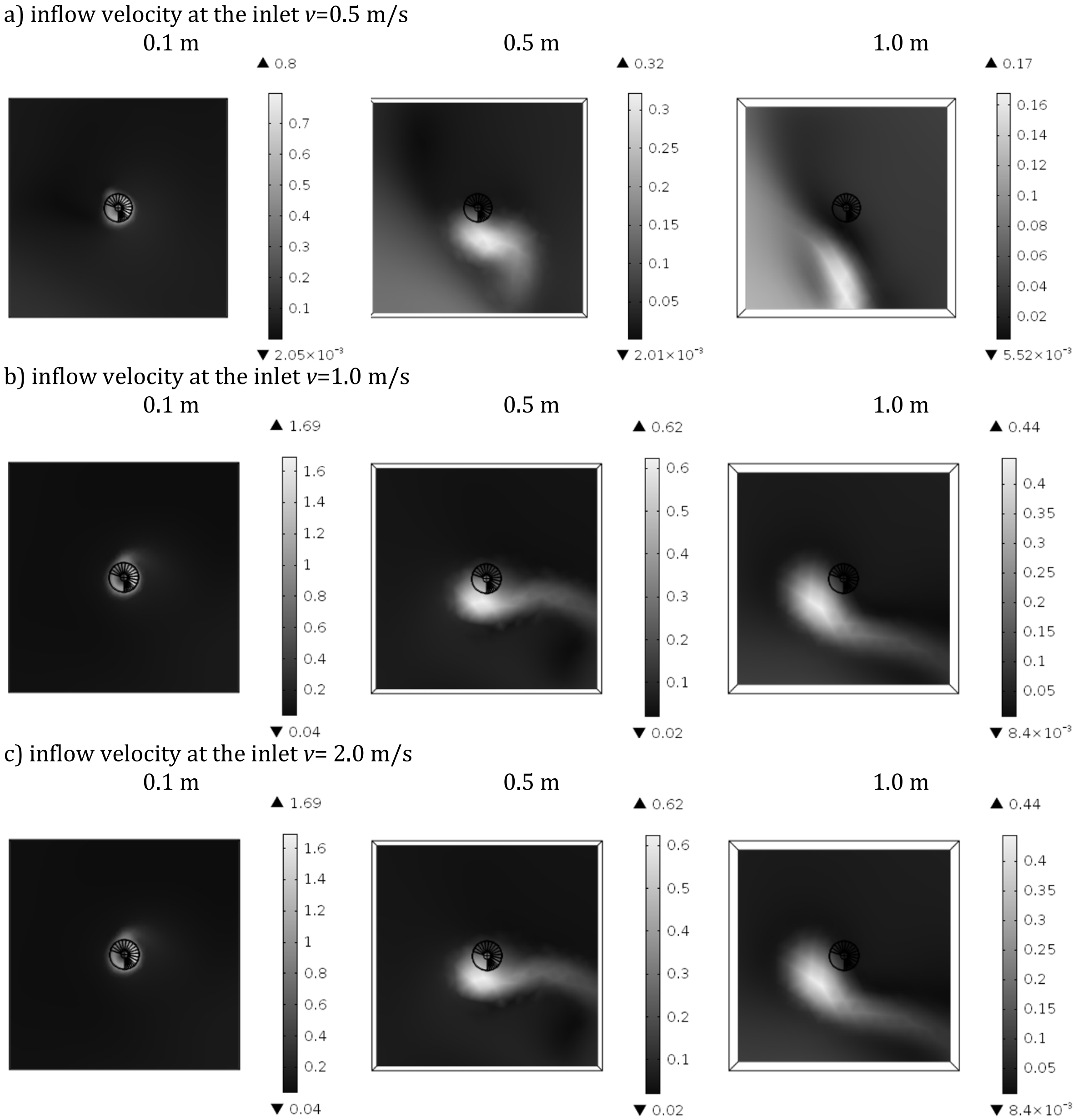

Figure 6. Slice views of air velocity, v [m/s], in the distance of 0.1 m, 0.5 m and 1 m inside 3D 1m cubic box at the outflow side of the cylindrical duct with helicoidal resonator (n=0.695, s/d=1.976, d_m/d= 0.24, g/d=0.04) for three air flow velocities: 0.5 m/s (a), 1 m/s (b) and 2 m/s (c). View from the inlet side in normal direction to the duct central axis with visible edges of helicoidal resonator.

In Figure 7 are presented the 3D views of streamlines from 20 points of the air flow velocity field, v [m/s], for considered CFD model with helicoidal resonator inside cylindrical duct with 1 m cubic box at the outlet. The three-dimensional views are presented at the outlet side of considered model.

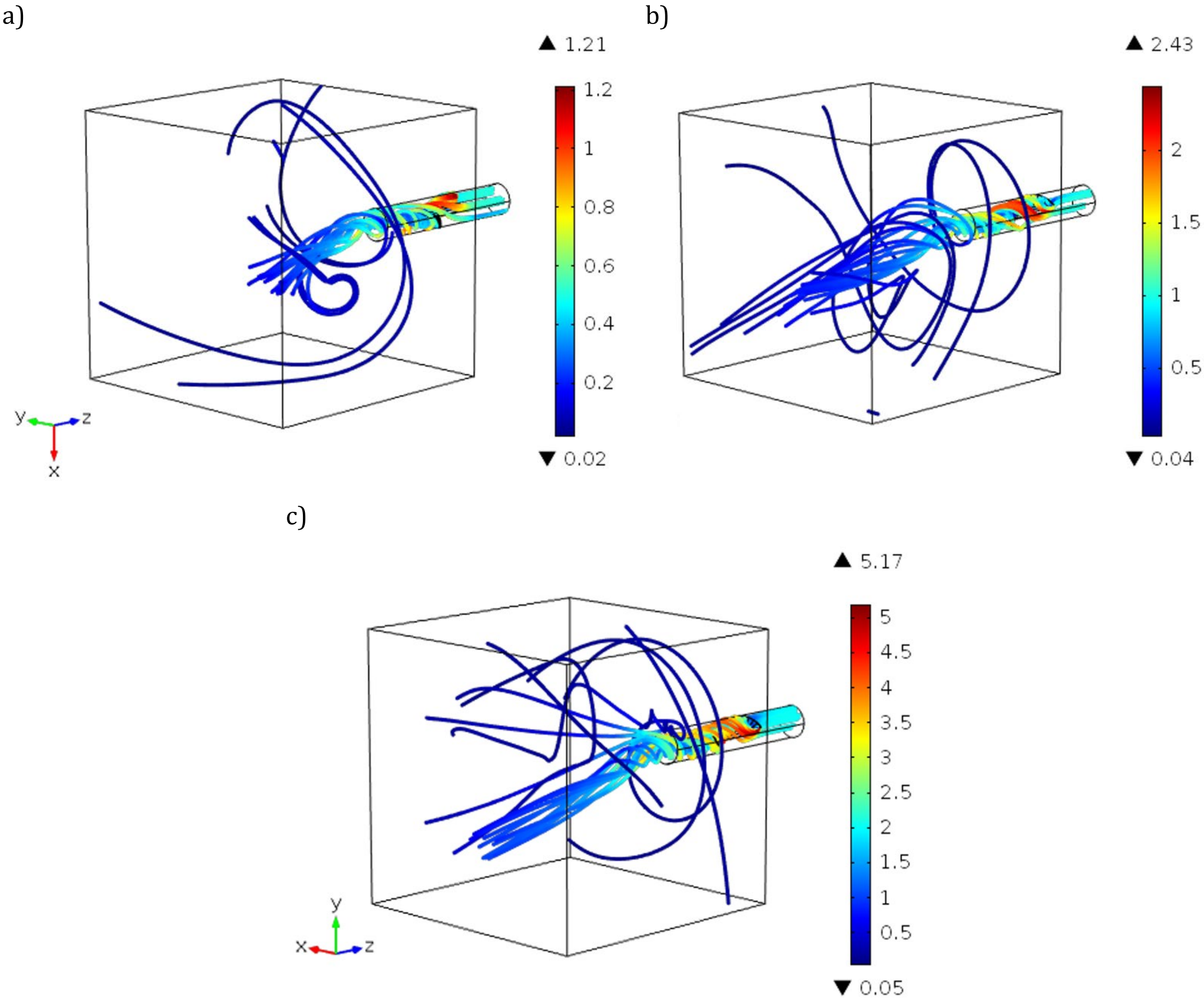

Figure 7. The 3D view of streamlines from 20 points of the air flow velocity field, v [m/s], for considered CFD model with acoustic helicoidal resonator (n=0.695, s/d=1.976, d_m/d= 0.24, g/d=0.04) inside cylindrical duct with 1 m cubic box at the outlet. Air flow velocities: a) v=0.5 m/s, b) v=1.0m/s, c) v=2.0 m/s. View from the outlet side – cubic box.

On the basis of the presented results of numerical tests of the considered acoustic helicoidal resonator, it can be seen that the higher air flow velocities in the outlet space are directed downwards for each considered air velocity at the inlet of the system. It should also be noted that at a distance of 0.1 m from the outlet of the cylindrical duct with a helicoidal resonator inside, higher flow velocities were noted than at the inlet of the system: for 0.5 m/s it was 0.8 m/s, for 1.0 m/s it was 1.69 m/s and for 2.0 m/s it was 3.83 m/s. Additional analysis of the numerical results showed that the mean flow velocity after the helicoidal resonator at the outlet of the cylindrical duct was greater than the assumed velocity at the inlet of the considered system. For example, for velocity that equals 1 m/s at the inlet, the mean velocity at the outlet of the pipe was 1.18 m/s, and for velocity that equals 2 m/s at the inlet, the mean velocity at the outlet of the pipe was 2.47 m/s. Therefore, it can be concluded that in the vicinity of the helicoidal resonator there is a local enhancement of the air flow velocity. Nevertheless, in any case, the swirls of the outgoing air stream visible on all numerical have an influence on its mixing with the air contained in the room.

4. Conclusions

This paper presented the results of experimental and numerical research examining the selected acoustic helicoidal resonator as the end element of the air installation.

Experimental tests of sound power levels of air-terminal devices were carried out in accordance with the PN-EN ISO 5135 and PN-EN ISO 3741 standards. Based on the results of measurements of acoustic power levels in one-third octave bands, it should be concluded that for each considered flow velocity, lower levels are visible in the one-third octave band with a center frequency of 1250 Hz, which corresponds to the resonant frequency of the considered helicoidal resonator (in this case, 1270 Hz). Thus, the noise generated by the air flow is damped by the action of the helicoidal resonator. Total sound power levels generally tend to increase with increasing flow velocity with the exception of 1 m/s and 4 m/s, which are higher than the following levels. For the highest analyzed flow velocity, 7 m/s, the sound power levels are clearly higher in the individual one-third octave bands. This is due to greater airflow noise due to greater turbulence as the flow velocity increases. The greatest discrepancies are visible for low air flow values, i.e. 1, 2 and 5 m/s. It is necessary to perform further tests related to the continuous flow tests in order to determine the sound attenuation characteristics as a function of the flow velocity. The tests should also be combined with tests of other helicoidal resonators with a different number of turns in order to determine or exclude the characteristics of helicoidal resonators.

The CFD turbulent model were solved with the use of single-phase flow k-ω turbulence RANS equations with compressible flow (Mach number less than 0,3) in COMSOL Multiphysics program. On the basis of the achieved results of numerical tests of the considered acoustic helicoidal resonator, it can be concluded that the higher air flow velocities in the outlet space are directed downwards for each considered air velocity at the inlet of the system. It should also be noted that at a distance of 0.1 m from the outlet of the cylindrical duct with a helicoidal resonator inside, higher local air flow velocities were noted than at the inlet of the system: for 0.5 m/s it was 0.8 m/s, for 1.0 m/s it was 1.69 m/s and for 2.0 m/s it was 3.83 m/s. Therefore, it can be concluded that in the vicinity of the helicoid resonator there is a local enhancement of the air flow velocity. Nevertheless, in any case, the swirls of the outgoing air stream visible on all numerical have an influence on its mixing with the air contained in the room. Thus, at the outlet of the ventilation system, the air stream can be directed depending on the angular position of the helicoidal resonator.

The performed tests are an introduction to the use of helicoidal resonator as end element of the air installation. At the same time, they introduce noise reduction in the installation, hence they can be simultaneously treated as a silencer. The undertaken direction of research will be continued due to the developmental nature.

Acknowledgments

This work was partially financed by the Polish Ministry of Science and Higher Education as a project No. 0612/SBAD/3588.

Additional information

The author(s) declare: no competing financial interests and that all material taken from other sources (including their own published works) is clearly cited and that appropriate permits are obtained.

References

1. A. Pełech; Wentylacja i klimatyzacja – podstawy; Oficyna Wydawnicza Politechniki Wrocławskiej, Wroclaw, Poland, 2008
2. Hideyuki Amai, Atila Novoselac; Experimental study on air change effectiveness in mixing ventilation; Building and Environment, 2016, 109, 101-111; DOI: 10.1016/j.buildenv.2016.09.015.
3. Ran Gao, Kaikai Liu, Angui Li, Zhiyu Fang, Zhigang Yang, Beihua Cong; Study of the shape optimization of a tee guide vane in a ventilation and air-conditioning duct; Building and Environment, 2018, 132, 345-356; DOI: https://doi.org/10.1016/j.buildenv.2018.02.006
4. Yu-Cheng Liu, Mihai G Burzo, Scott Sier, Cassandra Ellis; Improved thermal comfort of office occupants through better air diffuser designs; Proceedings of the ASME 2015 International Mechanical Engineering Congress & Exposition, IMECE2015, 2015, November 13-19, Texas, USA
5. Lei Wang, Xiahong Dai, Jianjian Wei, Zhengtao Ai, Yifan Fan, Lingling Tang, Tao Jin, Jian Ge; Numerical comparison of the efficiency of mixing ventilation and impinging jet ventilation for exhaled particle removal in a model intensive care unit; Building and Environment, 2021, 200, 107955; DOI: 10.1016/j.buildenv.2021.107955
6. M.H. Khairuddin, M.F.M. Said, A.A. Dahlan, K.A. Kadir; Review on resonator and muffler configuration acoustics; Archives of Acoustics, 2018, 43(3), 369-384; DOI: 10.24425/123909
7. W. Łapka; Tuning the selected acoustic helicoidal resonator with a short flat bar – numerical analysis; Vibrations in Physical Systems, 2019, 30(1), 2019140

8. W. Łapka; Numerical Analysis of Sound Propagation in Selected Acoustical System with Helicoidal Resonator Placed in Cylindrical Duct With 90 Degree Elbow; Vibrations in Physical Systems, 2018, 29, 2018018
9. W. Łapka; A three-dimensional finite element analysis of tuning the selected acoustic helicoidal resonator by the change of its mandrel diameter; Applied Acoustics, 2022, 185, 108443; DOI: 10.1016/j.apacoust.2021.108443
10. W. Łapka; Insertion loss of spiral ducts – measurements and computations; Archives of Acoustics, 2009, 34(4), 537-545
11. W. Łapka, C. Cempel; Computational and experimental investigations of a sound pressure level distribution at the outlet of the spiral duct; Archives of Acoustics, 2008, 33(4S), 65-70
12. W. Łapka; Numerical study of acoustic-structure interaction of selected helicoidal resonator with flexible helicoidal profile; Archives of Acoustics, 2018, 43(1), 83-92
13. W. Łapka, M. Szymański, R. Górzeński; The study of pressure drop depending on the air flow rate in duct of selected helicoidal resonators; Archives of Acoustics, 2013, 38(3), 442
14. W. Łapka; Rotating helicoidal resonators – pilot study; Archives of Acoustics, 2013, 38(3), 442
15. PN-EN ISO 5135:2020; Acoustics. Determination of sound power levels of noise from air-terminal devices, air-terminal units, dampers and valves by measurement in a reverberation test room, 2020
16. PN-EN ISO 3741:2011; Acoustics. Determination of sound power levels and sound energy levels of noise sources using sound pressure.Precision methods for reverberation test rooms, 2011
17. PN-EN 12238:2002; Ventilation for buildings. Air terminal devices. Aerodynamic testing and rating for mixed flow application, 2002
18. Comsol A.B., Comsol Multiphysics, CFD and Acoustics Module, User's Guide and Model Library, Documentation Set, Stockholm, Sweden, 2020
19. D.C. Wilcox; Turbulence Modeling for CFD, 3rd edition; DCW Industries Inc., La Canada CA, 2006
20. D. C. Wilcox; Formulation of the k-omega Turbulence Model Revisited; AIAA Journal, 2008, 46, 11, 2823-2838